

Reliability analysis of uncertain structures using earthquake response spectra

Abbas Moustafa*¹ and Sankaran Mahadevan²

¹*Department of Civil Engineering, Minia University, Minia 61111, Egypt*

²*Department of Civil & Environmental Engineering, Vanderbilt University, Nashville, TN 37235, USA*

(Received January 21, 2011, Revised March 7, 2011, Accepted March 11, 2011)

Abstract. This paper develops a probabilistic methodology for the seismic reliability analysis of structures with random properties. The earthquake loading is assumed to be described in terms of response spectra. The proposed methodology takes advantage of the response spectra and thus does not require explicit dynamic analysis of the actual structure. Uncertainties in the structural properties (e.g. member cross-sections, modulus of elasticity, member strengths, mass and damping) as well as in the seismic load (due to uncertainty associated with the earthquake load specification) are considered. The structural reliability is estimated by determining the failure probability or the reliability index associated with a performance function that defines safe and unsafe domains. The structural failure is estimated using a performance function that evaluates whether the maximum displacement has been exceeded. Numerical illustrations of reliability analysis of elastic and elastic-plastic single-story frame structures are presented first. The extension of the proposed method to elastic multi-degree-of-freedom uncertain structures is also studied and a solved example is provided.

Keywords: structural reliability; uncertainty; random damping; Monte Carlo Simulation; FORM; earthquake loads; response spectrum.

1. Introduction

The problem of reliability assessment of engineering structures under earthquake loads has received significant research attention (Bender and Perkins 1993, Wen 1995, Rackwitz 2002, Moller and Foschi 2003, Gupta and Manohar 2006, Abbas and Manohar 2005a, 2005b, 2007). This problem involves two main sources of uncertainties, namely in the structural properties and the ground motion. The structural uncertainty arises due to natural variability, data limitations, and modeling assumptions with respect to the geometry, boundary conditions, and constitutive behavior of the material. The uncertainty associated with the earthquake load can be grouped into two categories, namely, those associated with the long term features (e.g. frequency, magnitude, time, location of occurrence, fault mechanism and soil amplification) and those associated with the details of the ground motion (e.g. duration, amplitude, frequency content and non-stationary trend). The first type of seismic uncertainty can be tackled by using predictive or physical models for ground motions (Brune 1970, Boore 1983) or using the seismic (deterministic or probabilistic) hazard

* Corresponding author, Ph.D., E-mail: abbas.moustafa@eng.miniauniv.edu.eg

analysis (SHA) of the site (Cornell 1968, McGuire 1995, Wen and Wu 2001). The seismic hazard at a given site is generally quantified in terms of the probability of exceedance of the design level peak ground acceleration and the probability of exceedance of the specified ground motion response spectral shapes (Boore 1983, Wen and Wu 2001).

The second type of earthquake uncertainty can be handled using well established random vibration theory (Abbas and Manohar 2005a, 2005b, 2007, Lin 1967, Nigam 1983). In seismically active regions, great earthquakes will produce large structural deformations and stresses. However, the probability of occurrence of such earthquakes within the life of the structure is very low. To account for this uncertainty in seismic-resistant design, a dual criteria of two level design earthquakes is often adopted (Collins 1995, Chopra 2007). The problem of reliability assessment of structures driven by time-variant loads is known as time-variant reliability problem and is properly studied in the literature (Bender and Perkins 1993, Wen 1995, Rackwitz 2002, Moller and Foschi 2003, Gupta and Manohar 2006). We consider the same problem but from a different perspective. Specifically, we consider the time-variant reliability assessment of uncertain structures driven by earthquake loads that are defined using the response spectra (RS). The proposed methodology takes advantage of the RS and thus does not require explicit dynamic analysis of the actual structure.

Variability in structural properties can be effectively tackled by using the stochastic finite element method (SFEM) (Haldar and Mahadevan 2000). Studies in this direction combine random vibration theory with SFEM (Manohar and Ibrahim 1999) or by considering the seismic loads as being deterministic (Muscolino *et al.* 2000). Comprehensive reviews on quantification and modeling of uncertainties involved in structural reliability analysis, component and system reliability and different reliability methods (e.g. FORM, SORM, importance sampling and adaptive importance sampling techniques, response surface method and Monte Carlo Simulation method) can be found in Rackwitz (2002), Gupta and Manohar (2006), Abbas and Manohar (2007), Muscolino *et al.* (2000), Ang and Tang (1984), Haldar and Mahadevan (2000). Other sources of uncertainties (e.g. data limitations, modeling assumptions, and human errors) are also significant and have been studied earlier (Ditlevsen 1981, Grigoriu 1984, Nowak 1986).

Earthquake loads are specified for design purposes of structures (1) in terms of the time history of the ground acceleration, (2) by modeling the ground acceleration as a random process; or (3) by specifying the response spectrum of the site.

The RS method is the most common approach for specifying seismic loads in structural design practice. Seismic hazard analysis is an efficient tool for specifying ground motions at a site compared to deterministic RS method. This is because SHA reflects influence from damaging earthquake events at all possible locations that may occur with a certain probability during the lifetime of the structure. In general, the uniform hazard response spectra (UHRS) which represent uniform probabilities of spectral amplitude exceedance during a specified time period is developed first. Subsequently, the design spectra are constructed on the basis of the UHRS (Cornell 1968, McGuire 1995, Wen and Wu 2001). In structural reliability studies so far, the earthquake loads have been usually modeled as time histories or random processes. This paper develops a probabilistic framework for seismic reliability analysis of structures with random properties using the response spectrum, thus avoiding the need for explicit dynamic analysis of the actual structure.

The present paper develops a methodology suitable for alternative levels of uncertainty modeling, specifically (a) uncertainties in only the structural parameters affecting its natural frequencies, (b) additional uncertainties in the seismic loading, and (c) additional uncertainty in damping of the structure. Thus, if a deterministic response spectrum is used to describe the seismic load, Model I

can be used. Model II suits uncertain structures subjected to seismic loading defined by a probabilistic response spectrum. Model III is the same as Model II but with randomness in the structure’s damping also included. Therefore, Model III includes randomness in the structural properties including damping and the earthquake load. Numerical illustrations on seismic reliability analysis of elastic and inelastic single-story frame structures with uncertain natural frequency, damping, loading and member strengths are provided. The extension of the proposed methodology to elastic uncertain multi-degree-of-freedom (MDOF) structures is studied and a solved example is presented.

2. Reliability analysis of SDOF structures using response spectra

2.1 Earthquake response spectra for the site

The seismic load can be specified using deterministic RS or by using the probabilistic hazard spectra of the site. In general, the deterministic RS of the site is estimated through the dynamic analysis of the single-degree-of-freedom (SDOF) system (Chopra 2007). Herein, a set of past recorded ground motions are normalized and the maximum response of the SDOF system is computed for each record. The dynamic analysis is repeated for a set of SDOF systems that span the frequency bandwidth of interest and the spectra of the site are computed by statistical analysis. Inelastic RS for the site is established by considering the nonlinear behavior of the SDOF systems. Fig. 1 depicts the nonlinear SDOF system and the force-displacement law for bilinear hysteretic systems. These procedures are standard and their details are provided in many references, see, e.g. (Chopra 2007). Design and hazard response spectra are also specified in building codes (IBC 2003, ASCE 2003).

2.2 Problem statement and solution procedures

In the present study, the earthquake load is assumed to be defined in terms of the response spectrum of the site and it is required to estimate the structural reliability under this type of definition of seismic loading. To do this, we first define the performance function given as

$$g(R, S) = R - S \tag{1}$$

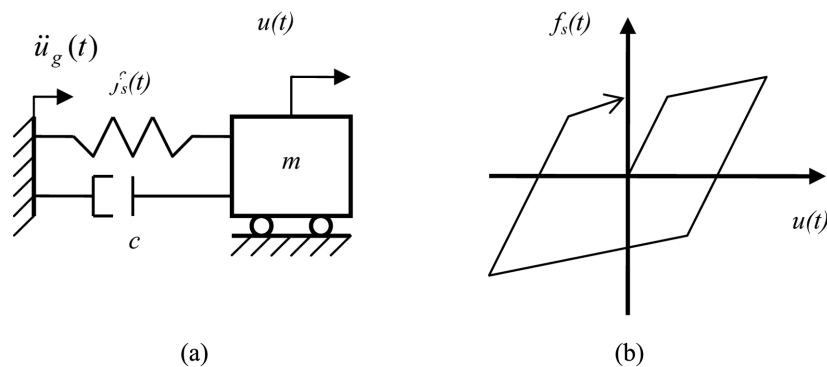


Fig. 1 (a) Bilinear hysteretic SDOF system and (b) force-displacement relationship

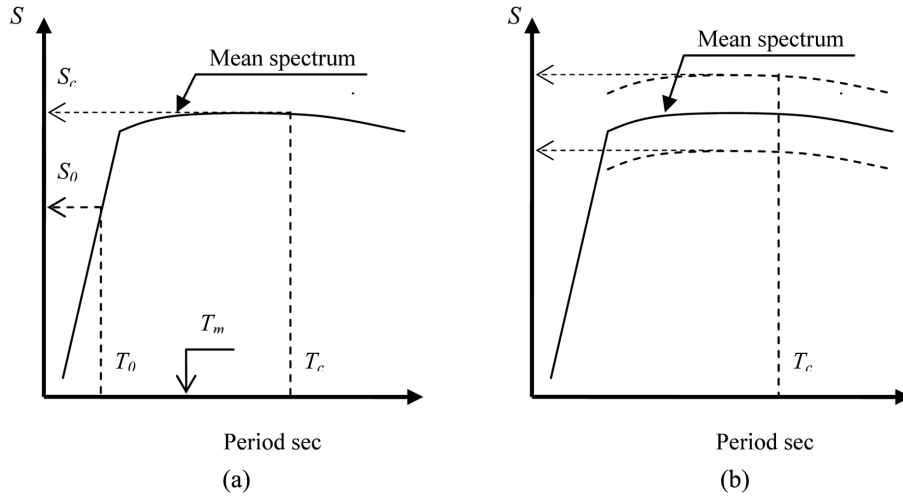


Fig. 2 Scatter in S due to (a) scatter in natural frequency and (b) scatter in seismic load

Here R is the resistance (or the capacity), a threshold value for a given response quantity of the structure (e.g. maximum permissible displacement, force or stress resultant at a point) and S is the demand (or load effect) associated with the earthquake load. $g(R, S) < 0$ defines the unsafe region, $g(R, S) > 0$ defines the safe region and $g(R, S) = 0$ represents the limit state that separates safe and unsafe zones.

The resistance R relates to the structural parameters (e.g. member cross-sections, modulus of elasticity, member strengths and mass), and S incorporates both the structural parameters and the earthquake load. Fig. 2 demonstrates schematically these two types of uncertainty. The randomness in the structure natural frequency (caused by randomness in the structure properties except damping which is studied later) causes scatter in the horizontal direction around the mean natural frequency μ_ω (Fig. 2(a)). The uncertainty in the seismic load causes scatter in the vertical direction around the mean spectrum (Fig. 2(b)). In this paper we consider two different models. Model I accounts for uncertainty in the structural parameters only (excluding damping) and Model II accounts for uncertainty in the structural parameters as well as uncertainty from the seismic load. The next two sections develop these two models.

2.2.1 Model I: Uncertainty in the structural parameters

This model tackles uncertainty due to randomness in the structural parameters only (except damping, which is considered in section 4). Herein, the site response spectrum is taken to be specified in terms of a single curve (e.g. the design spectrum computed from the SHA of the site or the mean spectrum, mean $+\sigma$, etc.) The structure natural frequency ω is taken as a random variable, and thus S turns out to be a random variable which is a function of ω . Randomness in ω could result from randomness in members cross-sections, modulus of elasticity, member strengths or mass. The performance function in Eq. (1) is rewritten as

$$g[R, S(\omega)] = R - S(\omega) \quad (2)$$

To demonstrate how $S(\omega)$ is quantified from a given response spectrum, we define the frequency

range of interest (ω_0, ω_c) of the structure associated with its fundamental natural frequency ω . For instance, assuming the structure natural frequency to be a random variable, we define $\omega_0 = \mu_\omega - f\sigma_\omega$ and $\omega_c = \mu_\omega + f\sigma_\omega$ where f is a constant. Subsequently, the associated response $S(\omega_0, \omega_c)$ spectrum range defines $S(\omega)$. The structural failure probability is thus computed as follows

$$P_f = P[R - S(\omega) < 0] = \iint_{g[R, S(\omega)] < 0} f_{RS}(r, s) dr ds \tag{3}$$

where $f_{RS}(r, s)$ is the joint probability density function of R and $S(\omega)$. Herein, R could be a function of the uncertain structural properties or the allowable value in the limit state specified by the analyst (e.g. maximum allowable stress or displacement). Specifically, in the current paper, the structural failure is estimated using a performance function that evaluates whether the maximum displacement has been exceeded.

Fig. 3 shows the displacement response spectrum for a site with stiff soil condition. The two dashed lines mark the period range $T_0 = 0.10$ sec and $T_c = 1.00$ sec ($\omega_0 = 6.28$ and $\omega_c = 62.83$ rad/sec) and the associated range of response spectrum $S(\omega)$ is shown on the vertical axis. The structural reliability computed using the numerical integration of Eq. (3) is referred to as Model 1a in the numerical analysis.

If the integration in Eq. (3) is difficult, then the structural failure probability may be estimated in terms of the reliability index β using first-order or second-order approximations of the limit state, or through Monte Carlo Simulation. The problem of determining the reliability index of the structure for performance functions such as that of Eq. (2) is well established in the literature (Ang and Tang 1984, Haldar and Mahadevan 2000). In the present paper we use the First Order Reliability Method (FORM) to estimate the reliability index. This involves transforming the non normal correlated random vector $\mathbf{X} = [R \ S(\omega)]^t$ into an equivalent uncorrelated standard normal space $\mathbf{X}^N = [X_1^N \ X_2^N]^t$ using the Rosenblatt or the Nataf transformation (Ang and Tang 1984, Haldar and Mahadevan 2000). This is followed by computing the reliability index as the shortest distance from the origin to the limit state. This procedure is standard and the details can be found in (Ang and Tang 1984, Haldar and Mahadevan 2000). The structural reliability computed using FORM is referred to as Model 1b here.

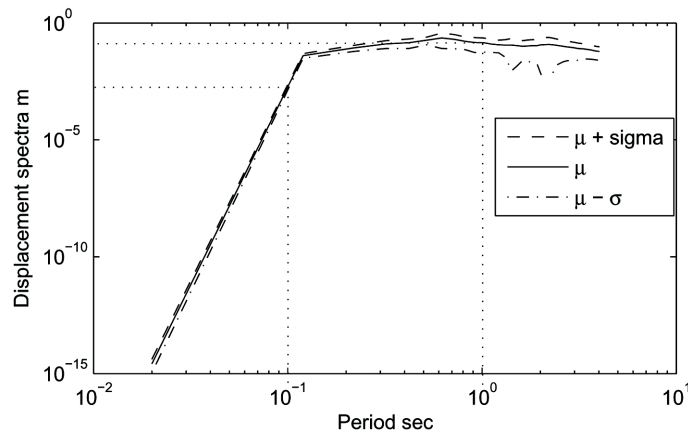


Fig. 3: Elastic response spectrum for a stiff site, $\zeta = 3\%$

2.2.2 Model II: Uncertainty in the structural parameters and seismic load

This model accounts for the uncertainty associated with the definition of the site response spectrum as well as randomness in S due to uncertainty in the structural natural frequency. The computation of the structural failure probability is carried out using numerical integration of Eq. (3). The steps involved in this calculation are summarized as follows:

1. Specify the mean and variance of the site response spectrum based on the damping ratio.
2. Define the structure performance function.
3. Define the distributions of ω and R and compute the period range (T_0, T_c) as in Model I.
4. Perform Monte Carlo Simulation to generate samples of S at each discrete period T_i using the data from step 1 and sort each set of numbers. The simulation is performed for the period range (T_0, T_c) .
5. Compute the CDF of S for each realization using numerical analysis (Haldar and Mahadevan 2000).
6. Determine P_f for each simulation as in Model I and average P_f across all the samples.

As mentioned earlier, the procedures outlined above account for the uncertainty associated with the specification of the site response spectrum and also due to randomness in the structure properties (affecting its natural frequencies).

3. Extension to MDOF uncertain structures

In this section we extend the formulation developed in the previous section on reliability analysis of uncertain SDOF systems to elastic MDOF systems with random properties. The structure properties such as cross-section dimension, modulus of elasticity, mass, and structural resistance are modeled as random variables. Again, the earthquake load is described in terms of the site response spectrum. Section 3.1 considers uncertainty in the structural parameters only (except damping) where a single response spectrum curve is used to describe the seismic load (e.g. response spectrum of a single component of ground acceleration or site mean response spectrum or mean $+\sigma$). Section 3.2 treats uncertainties in the structural parameters (except damping) as well in the seismic load. Section 3.3 addresses the extension to MDOF inelastic structures.

3.1 Model I: Uncertainty in the structural parameters

The performance function for a MDOF system (see Eq. (2)) is given in terms of the resistance R and the maximum modal responses as follows

$$g[R, S(\omega)] = R - S(\omega) = R - \sqrt{\sum_{i=1}^N \sum_{j=1}^N \rho_{ij} S(\omega_i) S(\omega_j)} = R - \sqrt{\sum_{i=1}^N \sum_{j=1}^N \rho_{ij} S_i S_j} \quad (4)$$

Herein S_i, S_j are the demands (random variables) for the i th and j th modes, respectively, ρ_{ij} is the correlation factor between the i th and j th modes, and N is the number of vibration modes retained in evaluating the structural response. Eq. (4) represents a nonlinear performance function that implicitly depends on the structure natural frequencies. The maximum total structural response as per the above equation is computed according to the complete quadratic combination (CQC) rule.

The CQC rule is known to provide an accurate estimate of the structure total response compared to other combination rules (e.g. the absolute summation (ABSSUM) and the square root of the sum of the squares (SRSS)) (Chopra 2007). This is because the CQC rule accounts for contributions from cross terms.

The CDF of each of the random variables S_i , $i = 1, 2, \dots, N$ are obtained from the site response spectrum. The quantification of the correlation matrix ρ is illustrated in the numerical examples. The performance function of Eq. (4) is an explicit nonlinear function of the set of correlated $N + 1$ random variables $\mathbf{X} = [R S_1 S_2 \dots S_N]^t$. Note that $g(\mathbf{X})$ implicitly depends on the structural parameters since S_1, S_2, \dots, S_N are functions of the structural parameters. In general, these random variables may be correlated and non normal. The evaluation of the structural failure probability is not straightforward as is the case with SDOF structures (Section 2.2). This is because the $N + 1$ dimensional joint probability density function of the random variate \mathbf{s} is usually not available, and the multi-dimensional integration is quite cumbersome. Therefore, the computation of an associated reliability index using FORM is pursued as in Model 1b of Section 2.2.1. The structural reliability is thus estimated based on the following condition

$$P[g(\mathbf{X}) < 0] = P\left[R - \sqrt{\sum_{i=1}^N \sum_{j=1}^N \rho_{ij} S_i S_j} < 0\right]; i, j = 1, 2, \dots, N \quad (5)$$

For linear limit state functions, as was the case for SDOF systems (see Eq. (3)), the computation of the reliability index is carried out in one step. On the other hand, the computation of the reliability index for nonlinear performance functions as Eq. (4) is an optimization problem which is solved iteratively. In the present study, the evaluation of the reliability index of the structure is carried out by using FORM (Rackwitz and Fiessler 1978). The values of the random structural parameters are generated using Monte Carlo Simulation.

The steps involved in these calculations can be summarized as follows:

1. Specify the site response spectrum based on the structure's damping ratio.
2. Define the structure performance function.
3. Define the distribution of the structural random properties (cross-section dimensions, Young's modulus, masses, resistance, etc.).
4. Perform Monte Carlo Simulation to simulate the structure random properties.
5. Carry out free-vibration analysis for each simulation.
6. Determine the maximum responses S_1, S_2, \dots, S_N associated with the computed natural frequencies and mode shapes for each realization, from the RS of step 1.
7. Estimate the CDF of S_1, S_2, \dots, S_N using numerical techniques.
8. Perform FORM analysis to compute the reliability index β . FORM analysis includes iterative computation of the reliability index (as the shortest distance from the origin to the failure surface in the standard uncorrelated normal space) until some convergence criteria on β and $g(\mathbf{X})$ are satisfied. These procedures are standard and the details can be found in references (Ang and Tang 1984, Haldar and Mahadevan 2000).

Thus the above algorithm contains two loops. In the outer loop Monte Carlo Simulation is used for generating numerical values for the structural random parameters. The inner loop uses FORM to evaluate the structural reliability index for each of the above simulations.

3.2 Model II: Uncertainty in the structural parameters and the seismic load

Herein, in addition to the uncertainty in the structural parameters (except damping), uncertainty in the seismic load is also considered. The same procedures of Section 3.1 are adopted with the important difference that the seismic load (step 1) is defined in terms of a probabilistic response spectrum. In step 6 of the previous algorithm the site response spectrum is used in an inner simulation loop (in the vertical direction) inside the main simulation loop (in the horizontal direction) to generate samples of the random variables S_1, S_2, \dots, S_N . CDF of these random variables (step 7) and reliability computation (step 8) are carried out for each sample. The reliability index β is computed for each realization and the final β is taken as the average across all the samples.

3.3 Extension to uncertain MDOF inelastic structures

The extension of the analysis to inelastic uncertain MDOF structures can be carried out as follows:

1. Use the site response spectrum to generate compatible time histories, see, e.g. (Iyengar and Rao 1979).
2. Generate random samples of the structure parameters and perform free vibration analysis for each sample.
3. Carry out nonlinear time history analysis for each simulated acceleration and compute the reliability index for each sample.
4. Average the reliability index across all samples.

If the seismic load is specified using probabilistic response spectra, the simulation is carried out for $S(\omega)$ as in Model II of Section 3.2. Note that the computational cost involved will increase since the inelastic response requires time history analysis for each simulation. Alternatively, one can approximate the MDOF inelastic structure with an equivalent SDOF inelastic system (Chopra 2007). This approach reduces the problem to that considered in Sections 3.1 and 3.2 (Models I and II). Note that, due to nonlinearity of the structure, the structural response is estimated using Monte Carlo Simulation and nonlinear time history analysis.

4. Uncertainty in damping of the structure

In the previous two algorithms (Sections 3.1 and 3.2) the structural damping was treated as a deterministic quantity. Quantification of damping is quite difficult, since unlike the inertial and stiffness properties of the structural system, damping does not refer to a unique physical phenomenon. The estimates of damping in a structural system have considerable uncertainty as a result of the complexity of damping mechanisms.

Information available from full-scale measurements for analyzing the variability of damping has been assembled by many researchers, see, e.g. (Haviland 1976, Davenport and Hill-Carroll 1986). A wide range of data for different response amplitude levels, structural systems and building heights were analyzed by Haviland (1976). This work showed that the log-normal and gamma distributions provide the best fit to the data. It also showed that the coefficient of variation of damping values varies between 42% and 87%. Davenport and Hill-Carroll (1986), based on analysis of available data from full-scale buildings, showed that the variability in damping varies between 33% and 78%

and suggested an average value of 40%. A comprehensive review on the dynamic response of structures with uncertain damping is presented in Kareem and Sun (1990).

In the present study, the treatment of damping as a random variable would add more complexity to the problem since the definition of the site response spectrum requires prior specification of the structure's damping ratio. Unlike randomness in other structural properties, random damping results in uncertainty in the site response spectrum in the vertical direction (see Fig. 2(b)). If past recorded ground accelerations at the site are available, the CDF of the site response spectrum can be estimated using Monte Carlo Simulation as follows:

- (1) Use the distribution function of the damping ratio to randomly generate a value of ζ .
- (2) Compute the response spectrum of the first record for this value of damping ratio.
- (3) Repeat steps 1 and 2 for all samples of the damping ratio.
- (4) Repeat steps 1-3 for all available acceleration records.
- (5) Use statistical analysis to estimate the CDF of the site response spectrum.

For instance, if N records are available and M simulations of damping ratio are generated for each record, the statistical analysis is carried out for $N \times M$ samples. Alternatively, analytical expressions from seismic codes combined with numerical simulation can be used in estimating the site response spectrum.

After developing the probabilistic response spectrum, the evaluation of the structural reliability follows the same procedure as in Section 3.2. Again, the random variables S_1, S_2, \dots, S_N are simulated (i.e. scatter along the vertical direction of Fig. 2) using the site response spectrum.

5. Numerical illustrations

5.1 Elastic single-story frame with random natural frequency

5.1.1 Structure considered

We consider a single-story frame structure with the natural frequency ω modeled as a normal random variable with $\mu_\omega = 1.50$ Hz and $\sigma_\omega = 0.25$ Hz. The structure is taken to behave linearly elastic when subjected to earthquake ground motion. The frequency range ($\omega_0 = 0.75$, $\omega_c = 2.25$) Hz, is determined with the parameter $f = 3.0$. The frame structure is taken to be located in a site with firm soil condition and a modal viscous damping is adopted ($\zeta = 0.03$ for Models I and II). The performance function of Eq. (2) is defined in terms of the maximum permissible displacement R and the actual maximum displacement $S(\omega)$. The resistance R is taken as a deterministic quantity of 0.10 m. The analysis is carried out for models I and II with constant damping and with random damping (Section 4) as will be demonstrated in Section 5.1.3.

5.1.2 Site response spectrum

A set of 20 earthquake ground motions are used in deriving the site response spectrum (COSMOS 2005, Abbas 2006). The minimum and maximum peak ground accelerations (PGA) of these records are 0.16 g and 0.47 g, respectively and the epicentral distance is less than about 30 km. The set of records are normalized such that each record possesses a peak acceleration of unity. The elastic displacement response spectrum of each record is computed. The site response spectra are computed by numerical analysis of all response spectra after these spectra are scaled to possess PGA of 0.20 g. Fig. 3 depicts the site elastic response spectrum with $\zeta = 0.03$. It may be noted that the selection

of records is primarily based on local soil conditions. The set of records must necessarily include all past records available for the site. In case a few past records are only available, then, recorded accelerograms from other sites that are geologically similar to the given site need to be added. It was observed however that the set of records provide a smooth Fourier spectra.

5.1.3 Results and discussion

Model I is considered first with the mean response spectrum (Fig. 3) defining the seismic load. The CDF of $S(\omega)$ is computed using numerical analysis. Fig. 4 shows the observed CDF for $S(\omega)$ and four fitted theoretical distributions to $S(\omega)$, namely, Normal, Log Normal, Gamma (Pearson type III), and Gumbel distributions. These theoretical distributions are computed for the purpose of investigating the shape of the actual CDF of $S(\omega)$. It is seen that the normal CDF is in close match with the observed CDF of $S(\omega)$ compared to other distributions. Note that the CDF of $S(\omega)$ depends on the structure parameters, the site soil conditions and the earthquake characteristics that are used in constructing the response spectrum. Thus, the CDF of $S(\omega)$ will automatically vary if any of these parameters are altered.

The K-S test was carried out for each of the four theoretical distributions for a significance level α and the maximum difference D_n is compared with the threshold value D_n^α . Thus, for the case of the normal distribution, and for a significance level $\alpha = 5\%$, the maximum difference $D_n = 0.07$ is less than the allowable value $D_n^\alpha = 0.21$.

Table 1 summarizes the numerical values of the failure probability computed using Model 1a from observed and theoretical distributions. The value of the parameter D_n for each of the fitted theoretical distributions is also listed in the table. Among the four theoretical distributions, the normal distribution gives the P_f value closest to the observed distribution.

The reliability index of the frame structure computed using Model 1b is 4.68 and the associated notional failure probability is 1.46×10^{-6} . Herein, $S(\omega)$ is assumed to be a normal random variable. The probability of failure computed from Model II is 5.53×10^{-5} which is seen to be higher than that computed from Model I. This is to be expected since Model II accounts for uncertainty in the site response spectrum unlike Model I.

To investigate the effect of including randomness in structural damping, ζ is assumed as a log-normal random variable with $\mu_\zeta = 0.03$, $\sigma_\zeta = 20\% \mu_\zeta$ and $\mu_\zeta = 0.03$, $\sigma_\zeta = 40\% \mu_\zeta$. A total of 20,000 samples response spectra (1,000 for each of the available 20 records) were employed in estimating the site response spectrum. Following the procedures described in previous sections, the failure

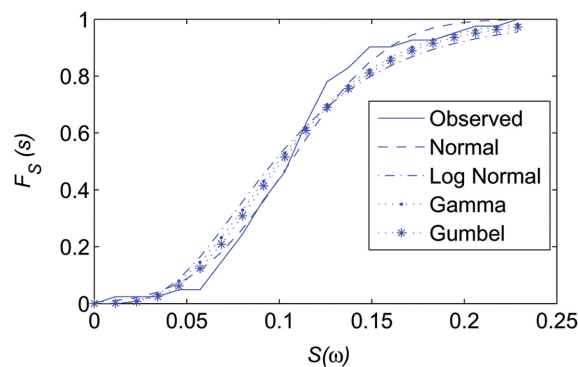


Fig. 4 Probability distribution function of $S(\omega)$ for elastic response spectrum

Table 1 Recorded ground motions used for estimating site response spectrum

Earthquake	Magnitude	Epicenter distance (km)	Component	PGA (m/s ²)	Intensity (m/s ^{1.5})	Site
Mamth Lakes 05.25.1980	6.2	1.5	W S	4.02 3.92	3.73 4.01	Convict Greek
Loma Prieta 10.18.1989	7.0	9.7	W S	3.91 4.63	3.82 5.22	Capitola
Morgan Hill 04.24.1984	6.1	4.5	S60E S30W	3.06 1.53	2.33 1.64	Halls valley
San Fernando 02.09.1971	6.6	27.6	N69W N21E	3.09 2.66	2.07 2.47	Castic old ridge
Parkfield 12.20.1994	5.0	9.1	W S	2.88 3.80	1.33 1.74	Parkfield fault
Caolinga 05.02.1983	6.5	30.1	W N	2.83 2.20	2.67 2.14	Cantua creek
Northridge 01.25.1994	6.7	5.9	S74E S16W	3.81 3.43	4.17 3.50	Canoga park
Cape Mendocino 04.25.1992	7.0	5.4	W S	3.25 2.89	2.44 2.31	Petrolia general
Westmorland 04.26.1981	5.0	6.6	E S	4.35 3.54	3.26 3.25	Westmorland
Imperial Valley 10.15.1979	6.4	17.4	S45W N45W	2.68 1.98	2.30 2.14	Calexico fire

probabilities from Models I and II with random damping are computed (Table 2). Model I with $\mu_\zeta = 0.03$, $\sigma_\zeta = 20\% \mu_\zeta$ and $\mu_\zeta = 0.03$, $\sigma_\zeta = 40\% \mu_\zeta$ reveals increase in P_f by about 11% and 17%, respectively than P_f for constant damping. Similarly P_f values from Model II are higher than P_f from constant damping by about 13% and 19%, respectively. These results reveal the influence of damping uncertainty on the structure failure probability.

An additional analysis, in which $S(\omega)$ is taken as the force in the spring and R is taken as the maximum permissible force in the spring was carried out. Herein, R is modeled as a normal random variable of mean $\mu_R = 0.225$ kN and standard deviation of 5% μ_R . For Model 1a, the probability of failure from observed CDF was computed as 4.37×10^{-7} while the reliability index from Model 1b was 4.45. For models I and II with random damping of $\mu_\zeta = 0.03$ and $\sigma_\zeta = 20\%$ the increase of associated values with constant damping were 10 and 14 %, respectively.

The parameter f which defines the range of the demand $S(\omega)$ was taken as 3. To investigate the effect of this parameter on the probability of failure of the structure, we varied this parameter and solved a new reliability problem. Thus, when $f = 2, 3, 4, 5$, β of Model Ib was computed as 4.81, 4.68, 4.56, 4.43. The small changes in β could be attributed to the small variation in $S(\omega)$ as can be seen in Fig. 3. The associated values for P_f from Model II were found to be 5.29×10^{-5} , 5.53×10^{-5} , 5.89×10^{-5} , 6.17×10^{-5} .

5.2 Inelastic single-story frame with random natural frequency

The frame structure of Example 1 is reconsidered but with the force-displacement relation modeled as elastic-plastic. A proportional viscous damping of 0.03 damping ratio is considered in this example. The natural frequency of the inelastic frame structure undergoing small displacement

$(u < u_y)$ is taken as that for the elastic structure of Example 1. The site inelastic response spectra were generated from past records following the procedures described in section 2 (see Fig. 1). In the numerical calculation, the inelastic displacement responses of the SDOF systems are computed using the Newmark- β method ($\beta = 0.25$ and $\Delta t = 0.005$ sec). For Model I, the displacement response spectrum for each normalized accelerogram is computed and the final spectrum is taken as the mean quantity across the set of 20 spectra and is scaled to PGA = 0.30 g. Fig. 5 shows the site mean inelastic response spectrum.

The performance function of Eq. (2) is considered with R taken as maximum permissible tip relative displacement ($R = 0.15$ m) and $S(\omega)$ the maximum displacement response defined by the site response spectrum. The observed and fitted theoretical Normal and Gumbel CDF for $S(\omega)$ are shown in Fig. 6. The numerical results are listed in Table 3.

Fig. 6 shows that the Normal distribution matches with the observed distribution of $S(\omega)$ better than the Gumbel distribution. However, the agreement of the normal distribution for the elastic spectra is relatively better than the case of inelastic response spectra ($D_n = 0.09$). Furthermore, a relatively larger number of distributions were possible to model $S(\omega)$ for the elastic case compared to the inelastic spectrum (here only two distributions satisfy the K-S test). P_f computed using Model 1a from observed distribution of $S(\omega)$ is 4.32×10^{-3} . The failure probabilities from the fitted Normal and Gumbel distributions were 9.06×10^{-3} and 9.78×10^{-3} , respectively. This implies that P_f from Normal distribution is closer to P_f from actual observed distribution.

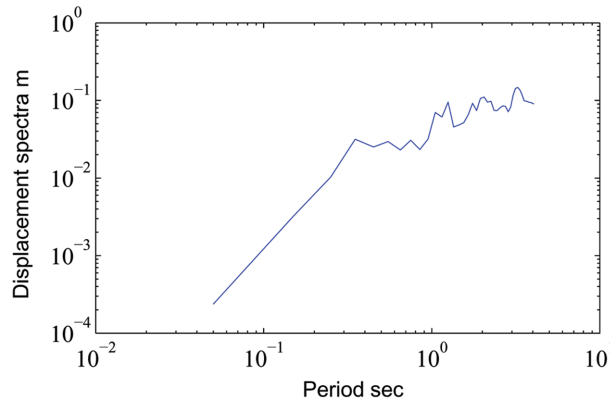


Fig. 5 Inelastic response spectrum for a stiff site, $\zeta = 3\%$

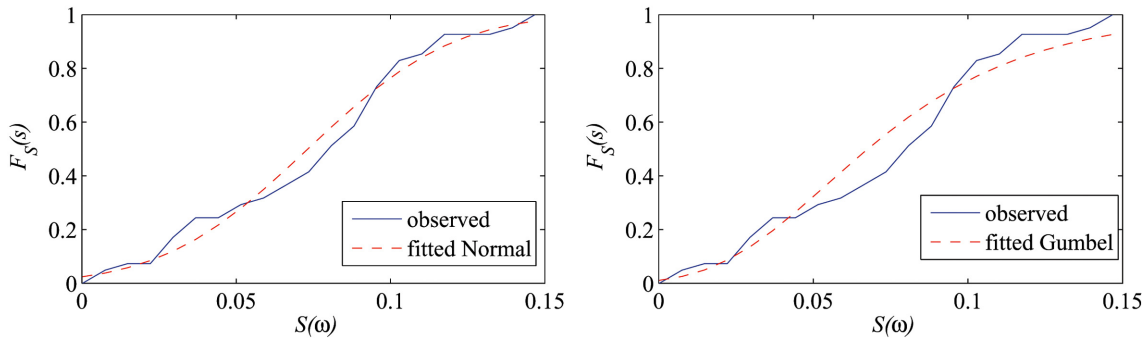


Fig. 6 Observed and theoretical PDF $S(\omega)$ for inelastic response spectrum

Table 2 Method 1a: P_f values from observed and fitted theoretical distributions ($\mu_R = 5 \times 10^4$ N, $\sigma_R = 5 \times 10^3$ N, $\zeta = 0.03$)

Parameter	Observed distribution	Fitted theoretical distribution			
		Normal	Lognormal	Gamma	Gumbel
P_f	4.62×10^{-7}	1.99×10^{-7}	1.76×10^{-7}	1.23×10^{-6}	1.16×10^{-6}
D_n	-	0.07	0.11	0.12	0.12

Table 3 P_f values for the uncertain elastic structure with random damping

Model	Model I (method 1a)			Model II (method 1b)		
	$\zeta = 0.03$ (determ.)	$\mu_\zeta = 0.03,$ $\sigma_\zeta = 20\% \mu_\zeta$	$\mu_\zeta = 0.03,$ $\sigma_\zeta = 40\% \mu_\zeta$	$\zeta = 0.03$ (determ.)	$\mu_\zeta = 0.03,$ $\sigma_\zeta = 20\% \mu_\zeta$	$\mu_\zeta = 0.03,$ $\sigma_\zeta = 40\% \mu_\zeta$
P_f	4.62×10^{-7}	5.14×10^{-7}	5.39×10^{-7}	5.53×10^{-5}	6.24×10^{-5}	6.57×10^{-5}

The reliability index of the structure from Model 1b is 2.14 and the associated notional P_f is 1.62×10^{-2} . Herein, $S(\omega)$ is assumed to be a normal random variable. Model II leads to $P_f = 4.65 \times 10^{-2}$ which is higher than that from Model I. The numerical results of this Example with random damping are given in Table 4. As in Example 1, the values of P_f with random damping are higher than those with constant damping.

5.3 Multi-story frame structure with random parameters

We consider the five-story reinforced concrete frame of Fig. 7(a). The frame structure has a span width $L = 9.00$ m and the floor height is $h = 4.00$ m. The modulus of elasticity is taken as a normal random variable of mean $\mu_E = 20$ Gpa and $\sigma_E = 2$ Gpa. The columns are assumed to have square cross-section of $\mu_a = 20$ m and $\sigma_b = 20$ m. The girders carry a normal random load of mean and standard deviation of 4.0, 0.40 KN/m, respectively.

The performance function of Eq. (5) is defined in terms of the tip relative displacement. Here, R

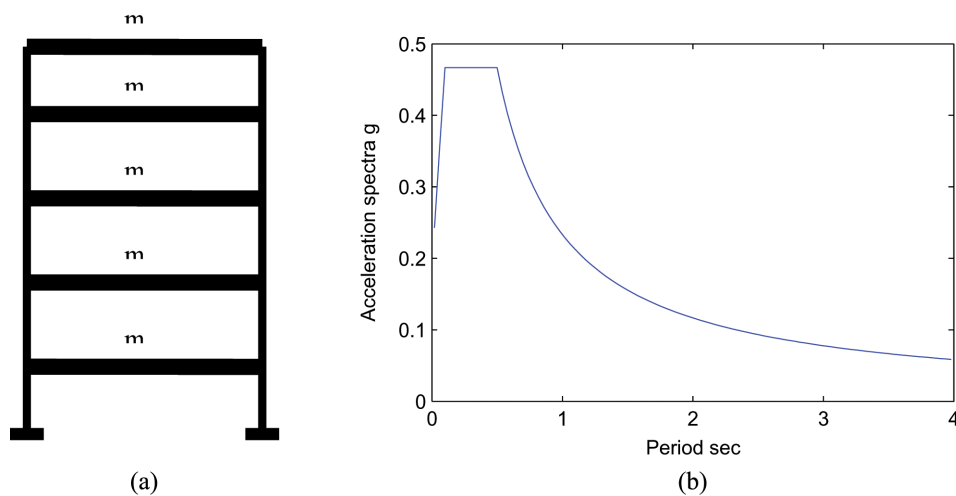


Fig. 7 (a) Multi-story concrete frame structure and (b) site response spectrum

is taken as a deterministic quantity ($R = 0.15$ m). The free vibration analysis is carried out for 5,000 samples and the mean and standard deviation for the first five natural frequencies of the structure were 1.51, 4.42, 6.97, 8.95 and 10.21 Hz and 0.26, 0.77, 1.21, 1.55 and 1.77 Hz, respectively. The number of random variables involved in this example is 9. The site response spectrum adopted for Model I of this Example is shown in Fig. 7(b) (IBC 2003, ASCE 2003). In Models I and II, ζ is taken as 5% for all the five modes.

The results computed from Model I are presented first. The mean values of modal demands S_1, S_2, S_3, S_4 and S_5 are 0.3049, 0.0302, 0.0084, 0.0026 and 0.0005 m, respectively and the associated standard deviations are 0.0547, 0.0054, 0.0015, 0.0005 and 0.0001 m, respectively. Note that these quantities are exact since the error associated with reading spectral ordinates is eliminated by computing these quantities from the mathematical expressions. To define the distribution functions for S_1, S_2, \dots, S_5 , the sampled data points for each of these random variables are used to estimate the underlying distribution function. The CDF for the first four modes are shown in Fig. 8. The figure shows also the normal distribution functions having the same mean and standard deviation computed from the sampled data points. Fig. 8 shows that S_1, S_2, \dots, S_5 follow normal distributions. The correlation coefficient matrix was computed as (Chopra 2007)

$$\rho_{ij} = \frac{\zeta^2(1 + \theta_{ij})^2}{(1 - \theta)^2 + 4\zeta^2\theta_{ij}}; \theta_{ij} = \frac{\omega_i}{\omega_j} \quad (6)$$

The correlation matrix (with $\zeta = 0.05$) is computed as follows

$$\rho = \begin{bmatrix} 1.0000 & 0.0104 & 0.0060 & 0.0049 & 0.0045 \\ 0.0104 & 1.0000 & 0.0477 & 0.0214 & 0.0158 \\ 0.0060 & 0.0477 & 1.0000 & 0.1390 & 0.0658 \\ 0.0049 & 0.0214 & 0.1390 & 1.0000 & 0.3676 \\ 0.0045 & 0.0158 & 0.0658 & 0.3676 & 1.0000 \end{bmatrix} \quad (7)$$

It is seen that the cross-correlation coefficients (off diagonal numbers) are small since the mean natural frequencies of the structure are well separated. In the numerical calculations, it was observed that the contributions to the maximum response of the structure from modes higher than the second mode are small. Following the procedures mentioned in Section 3, the set of correlated random variables are transformed into the uncorrelated standard normal space. Subsequently, β was computed to be 3.74 and $P_{f0} = 9.20 \times 10^{-5}$ (see Table 3). The sensitivity factors $\alpha_i, i = 1, 2, \dots, 5$ are computed as 0.9091, 0.4150, -0.0254, 0.0262 and -0.0008, respectively. These values indicate that the first two random variables S_1 and S_2 dominate β . If the SRSS rule is used in computing the peak total structural response (see Eq. (7)), β turns out to be 3.65 and if the absolute summation is employed $\beta = 3.60$. The value of β determined using SRSS is close to that computed using the CQC rule since the structure considered has well separated natural frequencies. The absolute summation leads to a lower value of β and thus overestimates P_f .

Model II (using CQC rule) leads to $\beta = 2.57$. As can be expected the notional P_f from Model II ($P_f = 5.09 \times 10^{-3}$) is higher than that computed from Model I. The number of simulations for the free vibration was taken as the same number used in Model I (5,000) and the number of the simulation for $S_1, S_2, \dots, S_5 = 10,000$. The standard deviation of the response spectrum was taken as 10 % of the

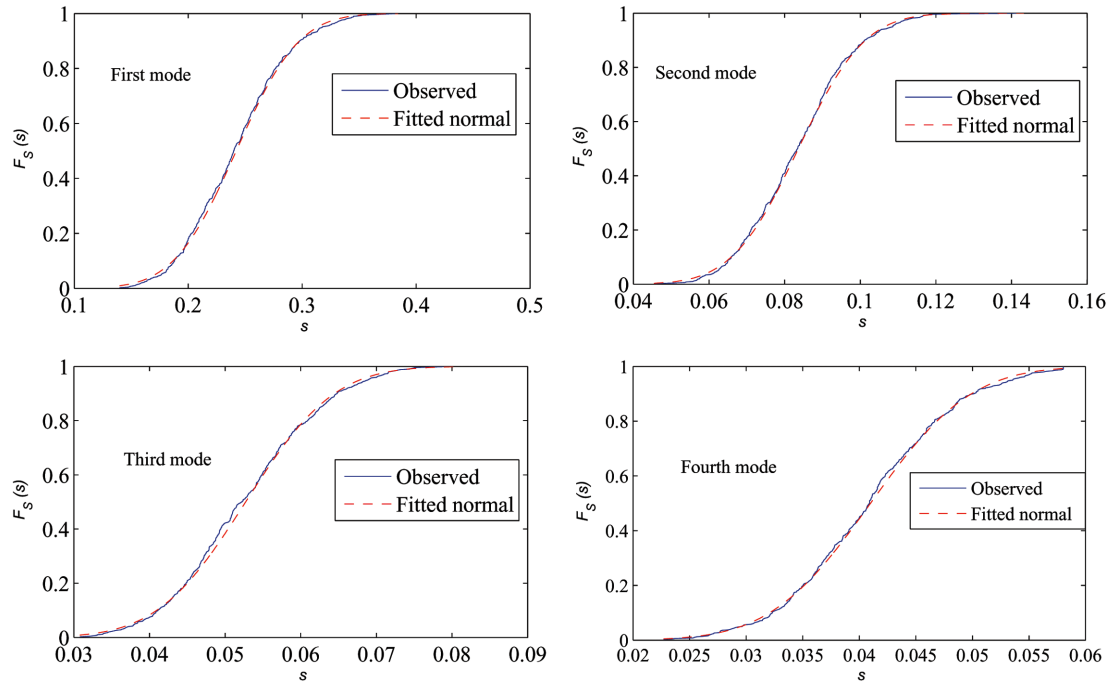


Fig. 8 Probability distribution function for S_i for the first 4 modes

Table 4 P_f values for the uncertain inelastic structure with random damping

Model	Model I (method 1a)			Model II (method 1b)		
	$\zeta = 0.03$ (determ.)	$\mu_\zeta = 0.03,$ $\sigma_\zeta = 20\% \mu_\zeta$	$\mu_\zeta = 0.03,$ $\sigma_\zeta = 40\% \mu_\zeta$	$\zeta = 0.03$ (determ.)	$\mu_\zeta = 0.03,$ $\sigma_\zeta = 20\% \mu_\zeta$	$\mu_\zeta = 0.03,$ $\sigma_\zeta = 40\% \mu_\zeta$
P_f	4.32×10^{-3}	4.83×10^{-3}	5.11×10^{-3}	4.65×10^{-2}	5.17×10^{-2}	5.45×10^{-2}

Table 5 Summary of β and associated notional P_f for the 5-storey frame structure

Model	Model I ($\zeta = 0.05$)			Model II ($\zeta = 0.05$)	Model II (CQC)	Model II (CQC)
	CQC	SRSS	ABSSUM	CQC	$\mu_\zeta = 0.05,$ $\sigma_\zeta = 20\% \mu_\zeta$	$\mu_\zeta = 0.05,$ $\sigma_\zeta = 40\% \mu_\zeta$
β	3.74	3.65	3.60	2.57	2.53	2.51
P_{f_0}	9.20×10^{-5}	1.31×10^{-4}	1.59×10^{-4}	5.09×10^{-3}	5.70×10^{-3}	6.04×10^{-3}

mean response spectrum of Fig. 7(b).

The reliability analysis of the structure with random damping using Models I and II were performed and the numerical results are given in Table 5. The results reveal that the values of P_f with random damping are higher than those with constant damping.

It may be emphasized that the use of SRSS and CQC for estimating the total response involves approximations. Obviously, the two methods combine the individual modal responses in two different ways. Neither of the methods gives the actual response and thus each of them has error. This is because the modal responses reach their peaks at different time instants while the total

response attains its peak at yet a different time instant. Furthermore, different forms of site response spectra (e.g. code spectra, probabilistic spectra, mean spectra) have been used in the analysis to demonstrate the applicability of the proposed formulation to alternative available response spectra.

6. Conclusions

A method for reliability analysis of structures with random parameters using the response spectrum is developed in this paper. The distribution of the structural demand is quantified from the site response spectra and thus explicit dynamic analysis of the actual structure is not required. The formulations developed account for uncertainty in the structural properties, such as, member cross-sections, material properties (modulus of elasticity, member strengths, mass, damping and strength characteristics) as well as in the seismic load. Numerical examples on the reliability analysis of elastic and elastic-plastic single-story frames, with random natural frequency and damping are presented. The extension of the formulations to uncertain elastic MDOF structures is also studied and a numerical example on reliability analysis of five-story frame structure is provided. The study uses Monte Carlo Simulation and takes advances of current advances in computations using computers.

The structural damping was modeled using viscous damping. The formulation developed in this study, however, is capable of handling other damping models (e.g. Rayleigh, Caughey, etc.). This can be done by determining the equivalent damping ratios from the parameters of the damping model and following the same procedures of the present study.

Acknowledgements

This study is partly supported by funds from the U. S. Air Force Research Laboratory through subcontract to General Dynamics Information Technology (Contract No. USAF- 0060-43-0001, Project Monitor: Mark Derriso). The support is gratefully acknowledged.

Rereferences

- Abbas, A.M. (2006), "Critical seismic load inputs for simple inelastic structures", *J. Sound Vib.*, **296**, 949-967.
- Abbas, A.M. and Manohar, C.S. (2005a), "Reliability-based critical earthquake load models. Part 1: Linear structures", *J. Sound Vib.*, **287**, 865-882.
- Abbas, A.M. and Manohar, C.S. (2005b), "Reliability-based critical earthquake load models. Part 2: Nonlinear structures", *J. Sound Vib.*, **287**, 883-900.
- Abbas, A.M. and Manohar, C.S. (2007), "Reliability-based vector nonstationary random critical earthquake excitations for parametrically excited systems", *Struct. Safety*, **29**, 32-48.
- Ang, A-H.S. and Tang, W.H. (1984), *Probability concepts in engineering planning and design*, Volume II Design decision, risk and reliability, John Wiley & Sons, NY.
- ASCE (2003), *Minimum design loads for buildings and other structures*, revision of ASCE-98. ASCE, Structural Engineering Institute.
- Bender, B.K. and Perkins, D.M. (1993), "Treatment of parameter uncertainty and variability for a single seismic hazard map", *Earthq. Spectra*, **9**(2), 165-195.
- Boore, D.M. (1983), "Stochastic simulation of high-frequency ground motions based on seismological models of

- the radiated spectra”, *B. Seismol. Soc. Am.*, **73**, 1865-1894.
- Brune, J.N. (1970), “Tectonic stress and the spectra of seismic shear waves from earthquakes”, *J. Geophys. Res.*, **75**, 4997-5009.
- Chopra, A.K. (2007), *Dynamics of structures*, 3rd Ed., Prentice Hall, NJ.
- Collins, K.R. (1995), “A reliability-based dual level seismic design procedure for building structures”, *Earthq. Spectra*, **11**(3), 417-429.
- Cornell, C.A. (1968), “Engineering seismic risk analysis”, *B. Seismol. Soc. Am.*, **58**, 1583-11606.
- COSMOS (2005), *Consortium organizations for strong-motion observation systems*, <http://db.cosmos-eq.org>.
- Davenport, A.G. and Hill-Carroll, P. (1986), “Damping in tall buildings; its variability and treatment in design”, *Building Motion in Wind, Proc.*, ASCE Convention, Seattle, WA.
- Ditlevsen, O. (1981), *Uncertainty modeling*, McGraw-Hill, New York.
- Grigoriu, M. (1984), *Risk, structural engineering and human error*, Editor, University of Waterloo Press, Canada.
- Gupta, S. and Manohar, C.S. (2006), “Reliability analysis of randomly vibration structures with parameter uncertainties”, *J. Sound Vib.*, **297**, 1000-1024.
- Haldar, A. and Mahadevan, S. (2000), *Probability, reliability and statistical methods in engineering design*, John Wiley and Sons, Inc., NY.
- Haldar, A. and Mahadevan, S. (2000), *Reliability assessment using stochastic finite element analysis*, John Wiley and Sons, Inc., NY.
- Haviland, R.A. (1976), “Study of the uncertainties in the fundamental translational periods and damping values for real buildings”, *Res. Rep. No. 5, pub. No. R76-12*, Dept of Civil Eng., MIT, Cambridge, MA.
- IBC (2003), *International building code*, International code council Inc., USA.
- Iyengar, R.N. and Rao, P.N. (1979), “Generation of spectrum compatible accelerograms”, *Earthq. Eng. Struct. Dyn.*, **7**, 253-263.
- Kareem, A. and Sun, W.J. (1990), “Dynamic response of structures with uncertain damping”, *Eng. Struct.*, **12**, 2-8.
- Lin, Y.K. (1967), *Probabilistic theory of structural dynamics*, McGraw-Hill, New York.
- Manohar, C.S. and Ibrahim, R.A. (1999), “Progress in structural dynamics with stochastic parameter variations: 1987-1998”, *Appl. Mech. Rev.*, **52**(5), 177-197.
- McGuire, R.K. (1995), “Probabilistic seismic hazard analysis and design earthquake: closing the loop”, *B. Seismol. Soc. Am.*, **85**, 1275-1284.
- Moller, O. and Foschi, R.O. (2003), “Reliability evaluation in seismic design: a response surface methodology”, *Earthq. Spectra*, **19**(3), 579-603.
- Muscolino, G., Ricciardi, G. and Impollonia, N. (2000), “Improved dynamic analysis of structures mechanical uncertainties under deterministic inputs”, *Probabilist. Eng. Mech.*, **15**, 199-212.
- Nigam, N.C. (1983), *Introduction to random vibration*, MIT press, London.
- Nowak, A.S. (1986), *Modeling human error*, Editor, ASCE, New York.
- Rackwitz, R. (2002), “Reliability analysis - a review and some perspectives”, *Struct. Safety* **23**, 365-395.
- Rackwitz, R. and Fiessler, B. (1978), “Structural reliability under combined random load sequences”, *Comput. Struct.*, **9**(5), 484-494.
- Wen, Y.K. (1995), “Building reliability and code calibration”, *Earthq. Spectra*, **11**(2), 269-296.
- Wen, Y.K. and Wu, C.L. (2001), “Uniform hazard ground motions for mid-america cities”, *Earthq. Spectra*, **17**(2), 359-284.